Top Curr Chem (2015) 365: 25–52
DOI: 10.1007/128_2014_555

Published online: 12 May 2014

Density Functional Theory Beyond the Generalized Gradient Approximation for Surface Chemistry

Benjamin G. Janesko

Abstract Density functional theory with generalized gradient approximations (GGAs) for the exchange-correlation density functional is widely used to model adsorption and reaction of molecules on surfaces. In other areas of computational chemistry, GGAs have largely been replaced by more accurate meta-GGA and hybrid approximations. Meta-GGAs and hybrids can ameliorate GGAs' systematic over-delocalization of electrons and systematic underestimate of reaction barriers. This chapter discusses extensions of meta-GGAs and screened hybrids to surface chemistry. It reviews evidence that GGAs' systematic underestimate of gas-phase reaction barriers carries over to reactions on surfaces, and that meta-GGAs and screened hybrids can improve results. It closes with recent applications and new work towards more accurate functionals for surfaces. These promising results motivate further exploration of meta-GGAs and screened hybrids for surface chemistry.

Keywords GGA • Meta-GGA • Reaction barrier • Screened hybrids • Surface chemistry

Contents

B.G. Janesko (✉)
Texas Christian University, 2800 S. University Dr., Fort Worth, TX 76129, USA
e-mail: b.janesko@tcu.edu

1 Introduction

1.1 Chemistry on Surfaces

Chemical reactions at surfaces and interfaces are central to many problems in chemistry. Topical examples include heterogeneous catalysis [1], surface-enhanced spectroscopies [2], battery technologies and hydrogen storage [3], and nanoscale devices [4]. Experimental studies of surface chemistry can be challenging. Measurements of molecules' adsorption, desorption, and reaction on single crystal surfaces under ultrahigh vacuum have yielded important insights [1] recognized by the 2007 Nobel Prize in Chemistry [5]. However, connections to practical surface chemistries often requires bridging the "pressure gap" between ultrahigh vacuum and industrially relevant high pressures, and the "materials gap" between single crystal surfaces and industrially relevant nanoparticles or catalysts. These gaps can play critical roles in surface chemistry. To illustrate, the Fischer–Tropsch process [6] for converting synthesis gas ($CO + H_2$) to long-chain hydrocarbons is catalyzed industrially by promoted and nanostructured cobalt [7] and iron [8] surfaces, but does not occur on single-crystalline surfaces under ultrahigh vacuum [9]. While there has been substantial progress in experiments bridging these gaps [10–12], experimental surface science remains challenging. Figure 3 of Maitlis [13] illustrates the contrast between well-defined experiments on homogeneous catalysts and the more "impressionistic" data available for heterogeneous catalysts.

1.2 Simulating Surface Chemistry

Simulations of molecules on surfaces have become essential tools for interpreting this impressionistic experimental data [14]. Such simulations typically require electronic structure calculations. Simulations of surface-enhanced spectroscopies combine classical electrodynamics models [15] with electronic structure calculations modeling how molecule–surface interactions shift a molecule's vibrational spectrum [16]. Simulations of nanoscale device chemistry generally center on modeling the electronic structure and properties of model devices [17]. Simulations of heterogeneous catalysis typically begin with electronic structure calculations on the geometries and adsorption energies of reaction intermediates on catalyst surfaces. The resulting potential energy surfaces can be applied in microkinetics models of reactions at realistic pressures, temperatures, and catalyst compositions [18–21].

Electronic structure calculations generally model a surface as either a periodic slab [22] or a finite cluster of surface atoms [23], potentially embedded in a simpler model background [24]. Cluster models are widely used for insulators, and are readily applicable to charged species. However, cluster models for metal surfaces often converge slowly with cluster size [25]. (Differences between calculations at different levels of theory can converge more rapidly [26].) Electronic structure approximations applicable to periodic slabs are desirable for treating metal, semiconductor, and insulator surfaces on an equal theoretical footing.

1.3 Choice of Electronic Structure Approximation

Electronic structure calculations on molecules, solids, and surfaces typically must approximate the many-body electron–electron interactions [27]. To be useful, an approximation should be both accurate enough to make experimentally meaningful predictions, and computationally inexpensive enough to treat the chosen system in a reasonable time using available computational resources. Several different electronic structure approximations have been applied to surfaces. One route uses first principles ab initio approximations for the many-electron wavefunction. Recent ab initio calculations on surfaces include coupled cluster [28–31] simulations of clusters of surface atoms, and quantum Monte Carlo (QMC) [26, 32–35] and random phase approximation (RPA) [36–42] simulations of periodic slabs. Unfortunately, ab initio methods typically have rather steep computational scaling [27], making them problematic for large and realistic model surfaces. A second route is to use tight-binding Hamiltonians. These can be applied to large systems, but require substantial empirical parameterization and can have limited transferability [43].

2 GGAs for Surface Chemistry

2.1 Density Functional Theory

The vast majority of electronic structure calculations on surfaces use Kohn–Sham density functional theory (DFT) [44, 45]. DFT can often provide acceptable accuracy at modest computational expense. Figure 1 illustrates DFT's dominance in modeling surface chemistry.

Kohn–Sham DFT models the ground state of an N-electron system as a reference system of N noninteracting Fermions corrected by a mean-field Hartree interaction,

$$E_{\mathrm{H}}[\rho] = \frac{1}{2}\int d^3\mathbf{r}\int d^3\mathbf{r}'\,\frac{\rho(\mathbf{r})\rho(\mathbf{r}')}{|\mathbf{r}'-\mathbf{r}|}, \tag{1}$$

and an exchange-correlation (XC) density functional $E_{\mathrm{XC}}[\rho]$ containing all many-body effects. $\rho(\mathbf{r})$ is the probability density for finding an electron at $\mathbf{r}$. The Kohn–Sham reference system has the same $\rho(\mathbf{r})$ as the real system by construction. The exact $E_{\mathrm{XC}}[\rho]$ is a unique and variational functional of $\rho(\mathbf{r})$ [44]. The Hamiltonian of the non-interacting Fermions includes local and multiplicative Hartree and XC potentials, e.g., $v_{\mathrm{XC}}(\mathbf{r}) = \delta E_{\mathrm{XC}}[\rho]/\delta\rho(\mathbf{r})$. Practical calculations typically use separate ↑- and ↓-spin densities and Kohn–Sham orbitals. This work suppresses spin dependence for conciseness. All orbitals, densities, density matrices, and exchange energies are assumed to be spin polarized.

The accuracy and computational expense of a typical DFT calculation is determined by the one-electron basis set used to expand the reference system's wavefunction, by any approximate treatments of relativistic effects, reciprocal space, and core electrons, and by the choice of approximate XC functional. DFT's success is

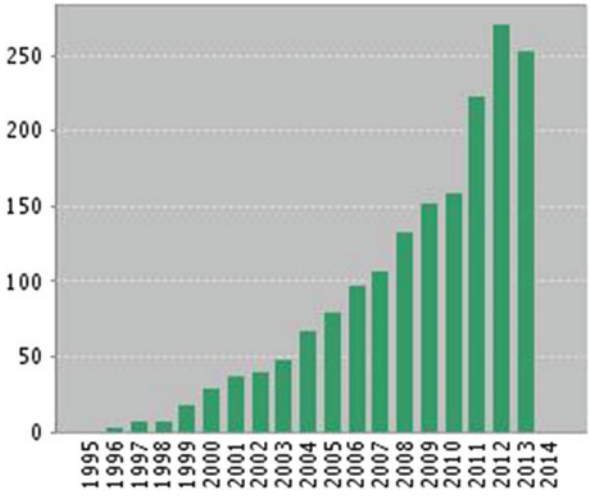

Fig. 1 Results of a Web of Science search for "DFT catalyst* surface*" illustrating published applications of DFT to heterogeneous catalysis [46]

largely attributable to the development of accurate and computationally tractable XC approximations [47]. Systematically convergent hierarchies of XC approximations (ab initio DFT) have been developed [48]. However, the vast majority of DFT calculations use an alternative "Jacob's Ladder" of approximations [49] based on the homogeneous electron gas (HEG, $\rho(\mathbf{r}) = \text{constant}$). The first "rung" of this ladder is the local spin-density approximation (LSDA) [50, 51] constructed to reproduce the numerically exact XC energy density [52, 53] of the HEG.

Generalized gradient approximations occupy the second rung of Jacob's Ladder. GGAs model the nonunique [54] XC energy density at point $\mathbf{r}$ as a function of $\rho(\mathbf{r})$ and its gradient:

$$E_{\mathrm{XC}}^{\mathrm{GGA}}[\rho] = \int d^3\mathbf{r}\, e_{\mathrm{XC}}^{\mathrm{GGA}}\left(\rho(\mathbf{r}), \left|\nabla\rho(\mathbf{r})\right|\right). \tag{2}$$

GGAs tend to improve upon the LSDA for total energies, atomization energies, and reaction barriers, and expand and soften bonds to (over)correct the LSDA's overbinding [55]. Their improved accuracy and computational simplicity makes them widely applied to periodic slab models for surfaces.

2.2 Design of GGAs

Unlike the LSDA, there is no single "best" choice of a GGA [55]. This flexibility has been exploited to construct GGAs which perform well for specific aspects of surface chemistry. In practice, a GGA's performance is often largely a function of its exchange enhancement factor F_{X}:

$$E_{\mathrm{X}}^{\mathrm{GGA}}[\rho] = \int d^3\mathbf{r}\, C_{\mathrm{X}}\rho^{4/3}(\mathbf{r})F_{\mathrm{X}}(s). \tag{3}$$

The "exchange" portion of $E_{\mathrm{XC}}[\rho]$ (4) is defined in terms of the expectation value of the electron–electron interaction operator, evaluated with the wavefunction of the noninteracting Kohn–Sham reference system [56]. Coefficient $C_{\mathrm{X}} = -\frac{3}{4}\left(\frac{6}{\pi}\right)^{1/3}$ is from the exact Kohn–Sham wavefunction of the HEG [57]. $s = |\nabla\rho(\mathbf{r})|/(2(6\pi^2)^{1/3}\rho^{4/3}(\mathbf{r}))$ is the unitless reduced density gradient.

Figure 2 illustrates representative GGAs' exchange enhancement factors and their performance for some properties relevant to surface chemistry. The LSDA is included for comparison. Similar to the LSDA, GGAs with small enhancement factors (PBEsol [62], AM05 [63], Wu-Cohen [64]) combine accurate lattice parameters with overestimated adsorption energies [65]. GGAs with larger enhancement factors (revPBE [66], RPBE [67], BLYP [68, 69]) improve adsorption energies [67] and molecular thermochemistry [70] at the expense of lattice parameters and geometries [71]. PBE [55] and PW91 [50, 72] provide intermediate performance

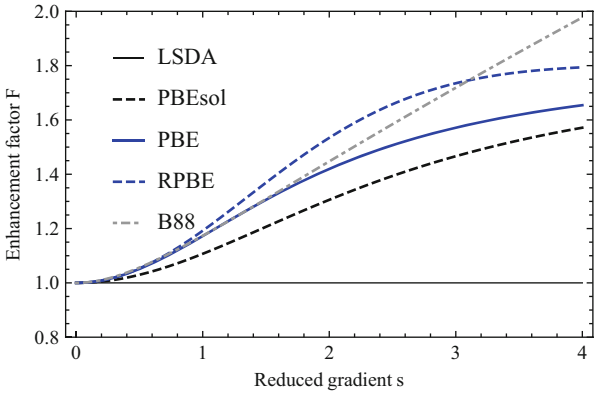

Functional	Lattice (pm) Ref. [58]	Bulk modulus (GPa)	CO/Pt(111) Eads (eV)	Barriers (kcal/mol)	GMTKN30 (kcal/mol)
LSDA	-4.59	35.74		17.5	12.0
PBEsol	-1.98	28.79	-2.1	13.2	7.4
PW91	1.95	7.46			
PBE	2.10	5.21	-1.6	10.5	5.2
RPBE,revPBE	4.19	-7.89	-1.3	8.1	4.5
BLYP			-1.0	9.6	5.3

Fig. 2 *Top*: Exchange enhancement factors of the LSDA and representative GGAs (F_X, Eq. (3)). *Bottom*: Mean errors in the shortest interatomic distances of 30 transition metals [58]; mean error in bulk moduli of 30 transition metals [58]; predicted chemisorption energies for CO on Pt(111) [60]; root-mean-square deviation in BH76 barrier heights and weighted mean absolute deviation in the GMTKN30 database of gas-phase properties (kcal/mol) [61]. Functionals are approximately sorted in order of increasing enhancement factor

[59]. None of these GGAs perform well for gas-phase reaction barrier heights, a fact central to what follows.

2.3 *Dispersion Corrected GGAs*

The locality of Eq. (2) prevents it from treating truly nonlocal correlation effects, including the asymptotic van der Waals interaction between distant closed-shell uncharged fragments [73]. Over the last decade, substantial resources have been invested into dispersion corrections for approximate XC functionals [74–76]. Dispersion corrections generally improve GGA simulations of molecule-surface adsorption [77], particularly for larger molecules such as coronene [78] and perylene derivatives [79, 80]. Dispersion corrections can be critical for some catalytic processes [37], some dissociation barriers [81], and some reactions of adsorbed molecules [82]. Dispersion corrections to adsorption energies are also important for apparent activation barriers on surfaces [83, 84]. However, dispersion

corrections generally do not correct GGAs' systematic underestimate of gas-phase reaction barriers. This can be seen, for example, in Tables S30–S31 of Goerigk and Grimme [85], where dispersion corrections slightly degrade PBE's performance for the BH76 benchmark set of gas-phase reaction barriers [85–87]. This assertion is supported by the widespread adoption of dispersion-corrected beyond-GGA functionals in computational chemistry [88–92]. Similar results are seen for reaction barriers of molecules on surfaces, evaluated with dispersion-corrected GGAs (Svelle et al. [93], Sect. 4). The studies reviewed below suggest that improving DFT for surface chemistry requires both dispersion corrections and beyond-GGA functional forms.

3 Successes of GGAs for Surface Chemistry

DFT calculations with generalized gradient XC functionals have been applied to an enormous array of problems in surface science. A comprehensive discussion of this literature would extend to several volumes, and is far beyond the scope of this work. This section presents a few representative successes connected to our work. Hafner [94], Greeley et al. [95], and Nørskov et al. [96] provide more extensive recent reviews.

GGAs are widely applied to determine how surface functionalization of nanostructures controls their properties. DFT calculations have mapped out the relationship between edge functionalization and electronic properties of graphene nanoribbons [4, 17, 97–99], have predicted how adsorbates open a bandgap in graphene electronics [100, 101], and have motivated studies of other quasi-1D semiconductors [102]. GGA calculations have also provided mechanistic insight into ammonia adsorption and reaction on Si(100) surfaces, a process relevant to chemical vapor deposition of silicon nitride for integrated circuits [103–107].

GGAs are also extensively applied to heterogeneous catalysis. Microkinetics models of ammonia synthesis over ruthenium nanoparticles, constructed from the RPBE and PW91 GGAs, reproduce experimental turnover frequencies to within an order of magnitude [108]. The calculated mechanisms also clarify the role of atomic steps for the rate-limiting N_2 dissociation [109]. Recent GGA calculations give new evidence for H_2-induced CO dissociation on Fischer–Tropsch catalysts [21, 110–114], a mechanism appearing to show significant structure sensitivity [115]. Studies of the C–C coupling step in the Fischer–Tropsch reaction point to the importance of surface carbide species [116]. Several recent simulations of the Fischer–Tropsch reaction considered the roles of adsorbed promoters which stabilize corrugated surfaces [117] and block graphitization [118], and adsorbed sulfur poisons which block CO dissociation [119]. These results have been expanded into complete microkinetics models of the Fischer–Tropsch reaction [21, 114, 120–123]. Other studies have considered methanol synthesis and the water-gas shift reaction [124] over some industrially relevant catalysts [18, 125, 126]. A recent combined computational and experimental study of methanation over nickel catalysts further

illustrates the value of GGA calculations for interpreting experiment [112]. GGA calculations have also provided atomic-scale explanations for the catalytic activity of gold nanoparticles, particularly bound to defective metal oxide supports [127–131]. Newer GGAs resolve the "CO/Pt(111) puzzle," in which standard GGAs' over-delocalization leads to qualitatively incorrect site dependence for CO adsorption on coinage metals [132]. Perhaps most importantly, GGA calculations have yielded general insights into periodic trends in adsorption [133, 134] and reactivity [135, 136] on catalyst surfaces.

A particularly interesting set of recent studies use GGA calculations to *design* new heterogeneous catalysts. Such studies often begin by identifying descriptors, such as adsorption or dissociation energies, which can be correlated with a catalyst's overall performance [137]. Typical calculations yield a "volcano plot" of catalytic activity vs descriptor, with optimal catalysts having intermediate values of the adsorption or dissociation energy [138]. GGA calculations of the descriptor on many model catalysts are then used to identify optimal candidates. GGA calculations on CO adsorption energies predicted that nickel-iron alloy catalysts could outperform more expensive pure Ni for CO methanation [139], a prediction subsequently verified by experiment [140]. GGA calculations were used to identify methylene chemisorption energies as a good descriptor for ethylene hydrogenation, and subsequently to identify novel nickel-zinc alloy catalysts [141]. GGA calculations on H_2 chemisorption energies were also used to identify near-surface alloy hydrogenation catalysts [142]. Nørskov et al. [143] reviews this active field.

4 Limitations of GGAs for Surface Chemistry

The successful applications reviewed above are all the more remarkable given the limitations of the GGA form. The large errors for gas-phase reaction barriers in Fig. 2 are not a special case, but are a general property of GGAs. GGAs systematically over-delocalize electrons [144–146] and overstabilize systems such as the stretched bonds of transition states. These errors are well known in the computational chemistry literature [86, 87, 147–154]. They have led to GGAs being almost entirely superseded in the computational chemistry community. (See, for example, the discussion of Fig. 1 in Burke [47].) The XC functionals which replaced them are discussed in Sect. 5.

The aforementioned difficulties of surface chemistry mean that there are relatively few experimental or computed benchmarks available to test GGAs' performance on surfaces. GGAs' limitations for surface chemistry are thus less well-characterized, and arguably less appreciated, than their limitations for molecules. However, available evidence strongly suggests that GGAs' errors for gas-phase barriers carry over to reactions of molecules on surfaces. The LSDA and the BP86 [50, 68] and BLYP GGAs underestimate QCISD(T) barriers for H_2 dissociation on

gas-phase silanes and a cluster model for Si(100) [155]. The PW91 GGA underestimates experimental [156] and quantum Monte Carlo [26] adsorption barriers for H_2 dissociative adsorption on Si(100). The PW91, PBE, and RPBE GGAs all underestimate the QMC barrier for H_2 dissociation on Mg(0001) [32]. PBE also underestimates QMC barriers for hydrogen abstraction by styrene radical on hydrogen-terminated Si(001) [33]. A series of studies by Bickelhaupt and coworkers show similar GGA errors for small organic molecules reacting with atomic Pd [157–159]. We found comparable errors in several GGAs' predicted dissociation barriers for H_2 dissociation on Au_3 and Ag_3 clusters [160]. The BP86 GGA severely underestimates completely renormalized coupled cluster reaction barriers for methanol oxidation on Au_8^- [31]. PW91 underestimates both coupled cluster reaction barriers for water splitting on an Fe atom, and RPA barriers for water splitting on Fe(100) [41]. PBE underestimates the barrier to O_2 sticking on a cluster model of Al(111) [161], and PBE and RPBE incorrectly predict barrierless O_2 dissociation on Al(111) slabs [162]. (While this is attributed to spin selection rules [162], recent hybrid DFT calculations [163] suggest that the GGA's limitations also play a role.) PBE and PW91 also incorrectly predict barrierless dissociation of H_2O_2 on cluster models of zirconium, titanium, and yttrium oxide surfaces [164]. Dispersion-corrected PBE calculations systematically underestimate the experimental reaction barrier to alkene methylation over a slab model zeolite catalyst [93]. We showed that the LSDA, the PBE, and revPBE GGAs underestimate the coupled cluster barrier for NH_3 dissociation on a cluster model of the reconstructed Si(100) surface, with differences between GGAs and beyond-GGA functionals persisting on larger clusters and periodic slabs [165]. GGAs also incorrectly predict the relative barriers to inter- vs intra-dimer NH_3 dissociation [104–106, 166, 167]. The LSDA and the PBE, PW91, and revPBE GGAs tend to underestimate diffusion Monte Carlo calculations for diffusion barriers (i.e., adsorption energies at different sites [168]) of adatoms on graphene [34, 169]. PBE also underestimates accurate reaction barriers for hydrogenation of graphene model compounds [30]. Other relevant GGA errors include overbinding of Cu on cluster models of the MgO(001) surface [170], and qualitatively incorrect spin distributions for defects on titania [171] and ceria [172] surfaces.

A particularly instructive illustration of GGAs' strengths and limitations comes from the aforementioned careful and insightful study of ammonia synthesis over ruthenium [108]. As discussed above, microkinetics models constructed from the PW91 and RPBE GGAs both predicted overall turnover frequencies within an order of magnitude of experiment. However, PW91 predicted that the rate-limiting N_2 dissociation barrier was 0.6 eV lower than the RPBE barrier. This corresponds to an enormous ten orders of magnitude discrepancy in the room-temperature Arrhenius rate constant. At least one of the predicted mechanisms thus enjoyed substantial error cancellation between inaccurate adsorption energies and reaction barriers. The authors explicitly characterized this error cancellation, stating that PW91 calculations "increased the coverage ... and decreased the number of free sites for dissociation" [108]. While such error cancellations are acceptable for some

applications, improvements are clearly desirable. This result illustrates the handicaps faced by computational surface scientists, and motivates the development of new approximations.

Several groups have attempted to remedy these issues with new GGAs. Some explore parameterized GGA forms similar to those pioneered in Becke [173]. The BEEF-vdW dispersion-corrected GGA incorporates 31 empirical parameters fitted using Bayesian error estimation [174]. Calculations using this functional accurately treat a wide variety of properties, from small-molecule heats of formation and noncovalent interactions to lattice constants, bulk moduli, and chemisorption energies [174]. Applications to metal–carbon bond formation from hydrogenation of supported graphene [175] and chemisorption on zeolites [176] leverage its strengths for noncovalent interactions. A study of CO_2 hydrogenation even points to improvements over RPBE for some reaction barriers on surfaces [177]. However, BEEF-vdW still gives a 0.26 eV mean absolute error in representative gas-phase reaction barriers [150], comparable to RPBE (0.27 eV), and significantly larger than the B3LYP global hybrid (0.17 eV) [174]. This is especially noteworthy given that B3LYP is, for a hybrid functional, not particularly accurate for reaction barriers. (To illustrate, the HISS screened hybrid discussed in Sect. 5.3 gives mean absolute errors of 1.7 and 1.8 kcal mol^{-1} in the HTBH38/04 and NHTBH38/04 test sets of gas-phase reaction barriers [86, 87], significantly smaller than B3LYP errors 4.23 and 4.34 kcal mol^{-1} obtained with a different computational setup [87].) The SOGGA11 [178] and non-separable N12 [179] GGAs, which respectively incorporate 18 and 24 empirical parameters, also give fairly large errors in these test sets [180]. These errors are dramatically reduced by the empirical meta-GGAs discussed in Sect. 5.4 [180].

"Specific reaction parameter" GGAs interpolating between, for example, PW91 and RPBE have also been proposed [181]. The interpolations are not guaranteed to be transferable, and require fitting to known experimental values. Interpolations can also be problematic where the known experimental value is not bracketed by two different GGAs [182]. GGAs' systematic underestimate of reaction barriers appears to make this circumstance rather common. Indeed, specific reaction parameter functionals originally tuned a hybrid functional's GGA term and fraction of exact exchange [183], exploiting the effects discussed in Sect. 5.1. Unfortunately, it appears that this "Procrustean dilemma" (Perdew et al. [62]) is an inherent limitation of the GGA form. This fact motivates exploration of methods beyond the GGA.

5 Beyond the GGA

DFT calculations on small and medium-sized molecules almost exclusively use beyond-GGA approximations for the exchange-correlation functional [47]. Extension of these methods to surface chemistry offers a potential solution to the

dilemma presented in Fig. 2. This section focuses on screened hybrids and meta-GGAs, two beyond-GGA approximations that show particular promise for surface chemistry.

5.1 Hybrid XC Functionals

DFT's widespread adoption for computational chemistry [47] is arguably directly attributed to the ability of fourth-rung "hybrid" XC approximations to outperform Hartree–Fock theory and second-order many-body perturbation theory for chemical bond breaking. Hybrid functionals [56] incorporate a fraction of exact exchange:

$$E_{\mathrm{X}}^{\mathrm{ex}}[\rho] = -\frac{1}{2}\int d^3\mathbf{r}\int d^3\mathbf{r}'\,\frac{\left|\gamma\left(\mathbf{r},\mathbf{r}'\right)\right|^2}{\left|\mathbf{r}-\mathbf{r}'\right|}. \tag{4}$$

Here, $\gamma(\mathbf{r},\mathbf{r}')$ is the nonlocal one-particle density matrix of the noninteracting Kohn–Sham wavefunction, constructed from the occupied orbitals of the Kohn–Sham wavefunction $\{\phi_i(\mathbf{r})\}$ as $\gamma(\mathbf{r},\mathbf{r}') = \Sigma_i\phi_i(\mathbf{r})\phi_i{}^*(\mathbf{r}')$. These orbitals and density matrices are thus implicit density functionals. Equation (4) provides the exact XC functional for one-electron systems, where it exactly cancels the Hartree interaction.

Admixture of a fraction of Eq. (4) to a GGA is justified by an adiabatic connection between the real system and the noninteracting Kohn–Sham reference [56, 184]. Such admixture corrects GGAs' over-delocalization, improving the prediction of a variety of properties including reaction barrier heights [146]. GGA calculations with more localized Hartree–Fock orbitals [153, 185], self-interaction corrections [186], and explicit constraints on localization [187] all give related improvements.

Hybrid functionals' success can be rationalized in terms of GGAs' simulation of nondynamical correlation [188]. Briefly, the many-body correction to the Hartree interaction may be modeled as a "hole" $h_{\mathrm{XC}}[\rho](\mathbf{r},\mathbf{r}')$ in the electron density about an electron at point $\mathbf{r}$ [145]. The total Hartree + XC energy becomes

$$E_{\mathrm{HXC}}[\rho] = \frac{1}{2}\int d^3\mathbf{r}\rho(\mathbf{r})\int d^3\mathbf{r}'\,\frac{\rho\left(\mathbf{r}'\right) + h_{\mathrm{XC}}[\rho]\left(\mathbf{r},\mathbf{r}'\right)}{\left|\mathbf{r}-\mathbf{r}'\right|}. \tag{5}$$

The XC hole is delocalized in systems such as stretched H_2^+, where $h_{\mathrm{XC}}[\rho](\mathbf{r},\mathbf{r}') = -\rho(\mathbf{r}')$. Nondynamical correlation in stretched covalent bonds localizes the XC hole about $\mathbf{r}$, such that (for example) an electron on the left atom in stretched singlet symmetric H_2 pushes the other electron to the right atom. GGA exchange functionals use localized exchange holes by construction. Thus, *GGA "exchange" in practice models both exchange and nondynamical correlation* [189].

Unfortunately, this rather crude model tends to overestimate nondynamical correlation and overbind. It is especially problematic in stretched H_2^+ and other

odd-electron bonds [190]. (Notions of self-interaction error [144, 191, 192], delocalization error [193], exact constraints on the XC hole [194], and symmetry breaking [195] provide additional insights into these effects.) Exact exchange admixture tunes this model, providing a surprisingly effective treatment of chemical bonding.

It is worth noting another useful aspect of hybrid functionals. Generalized Kohn–Sham calculations with a nonlocal XC potential $v_{\mathrm{XC}}(\mathbf{r},\mathbf{r}') = \delta E_{\mathrm{XC}}/\delta\gamma(\mathbf{r},\mathbf{r}')$ approximate the exact functional's derivative discontinuity, allowing occupied-virtual orbital energy gaps to better approximate fundamental band gaps better [196–198]. Kohn–Sham calculations with hybrid functionals require the local and multiplicative effective potential $\delta E_{\mathrm{X}}^{\mathrm{ex}}[\rho]/\delta\rho(\mathbf{r})$, typically constructed with optimized effective potential methods [199–201] or variants thereof [202]. Cohen et al. [197] provides a particularly useful illustration of the differences between Kohn–Sham and generalized Kohn–Sham calculations.

5.2 *Hybrid Functionals' Limitations*

Hybrid functionals have three limitations which are particularly relevant to surface chemistry. First, the optimal fraction of exact exchange is not known a priori, but depends on the role of nondynamical correlation in the system or property of interest. In practice, simple global hybrids typically require ~20% exact exchange for accurate thermochemistry [203, 204], ~40–50% exact exchange for kinetics [205], 100% exact exchange far from finite systems where Eq. (4) is the exact XC functional [206–208], and relatively small exact exchange admixtures for many organometallic properties [209, 210]. Figure 3 illustrates how this is problematic for reactions on metal surfaces. Other implications for surface chemistry are discussed in Hafner [211]. (The "+U" method, where the Kohn–Sham reference system includes a Hubbard repulsion on special sites [212], has similar issues centered on choosing the magnitude of U [213].) There has been substantial interest in overcoming this limitation through system-dependent [214–219] or position-dependent [220–222] exact exchange admixture, or through more sophisticated mean-field models of the XC hole [223, 224]. However, existing position-dependent "local hybrids" are not unambiguously more accurate than global hybrids [222, 225], and system-dependent exact exchange admixture can introduce size consistency issues [217].

Other limitations for surface chemistry arise from the long-range piece of exact exchange (large $|\mathbf{r}-\mathbf{r}'|$ in Eq. (4)) Evaluating this long-range contribution is computationally expensive in metallic systems where the Kohn–Sham $\gamma(\mathbf{r}, \mathbf{r}')$ delocalizes over a large range of $|\mathbf{r}-\mathbf{r}'|$ [226]. (More sophisticated treatments of this term have been proposed [227, 228].) Additionally, long-range exact exchange is exactly cancelled by higher order electron correlation effects in the HEG, and

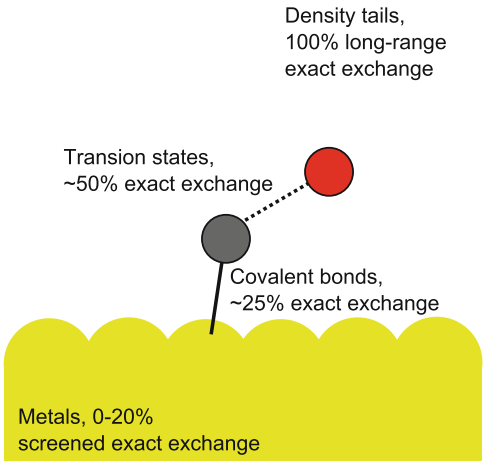

Fig. 3 Schematic of the optimal admixture of exact exchange in various regions of a reaction on a metal surface

approximately cancelled in metals [229, 230]. There are thus relatively few global hybrid DFT calculations on periodic metal slabs [161, 163, 231–233].

5.3 Screened Hybrids

Screened hybrid functionals [234, 235] rigorously [236] cut off the problematic long range of Eq. (4), sacrificing [237] an exact treatment of density tails [206–208] to enable facile treatments of periodic systems. The HSE06 screened hybrid [235, 238, 239] includes 25% of the error-function-screened exact exchange:

$$E_{\mathrm{X}}^{\mathrm{SR-ex}}[\rho] = -\frac{1}{2}\int d^3\mathbf{r}\int d^3\mathbf{r}'\,\frac{\left|\gamma\left(\mathbf{r},\mathbf{r}'\right)\right|^2}{\left|\mathbf{r}-\mathbf{r}'\right|}\mathrm{erfc}\left(\omega\left|\mathbf{r}-\mathbf{r}'\right|\right). \tag{6}$$

This is combined with 75% screened PBE exchange and 100% long-range PBE exchange and PBE correlation. Screened PBE exchange is constructed from explicit models [240, 241] of the angle- and system-averaged PBE exchange hole of Eq. (5):

$$E_{\mathrm{X}}^{\mathrm{SR-PBE}}[\rho] = \int d^3\mathbf{r}\, e_{\mathrm{X}}^{\mathrm{SR-PBE}}(\rho(\mathbf{r}),\nabla\rho(\mathbf{r})), \tag{7}$$

$$e_{\mathrm{X}}^{\mathrm{SR-PBE}}(\rho(\mathbf{r}),\nabla\rho(\mathbf{r})) = -\frac{1}{2}\rho(\mathbf{r})\int d^3\mathbf{r}'\,\frac{h_{\mathrm{X}}^{\mathrm{PBE}}\left(\rho(\mathbf{r}),\nabla\rho(\mathbf{r}),\left|\mathbf{r}-\mathbf{r}'\right|\right)}{\left|\mathbf{r}-\mathbf{r}'\right|}\mathrm{erfc}\left(\omega\left|\mathbf{r}-\mathbf{r}'\right|\right). \tag{8}$$

Exchange screening accelerates hybrid DFT calculations on periodic systems. Calculations with atom-centered basis functions can integrate $|\mathbf{r}-\mathbf{r}'|$ over a reduced number of replica cells [242]. Calculations with plane-wave basis functions can

downsample the k-space mesh for reciprocal space integration [226]. HSE06 is implemented in standard codes [243–245] and has been extensively applied to semiconductors [246, 247].

As for global hybrids, screened hybrids' optimum fraction of exact exchange and optimum screening parameter ω are not known a priori. The HSE06 exact exchange admixture comes from perturbation theory arguments [248], and the screening parameter is chosen empirically [235, 238]. Both parameters significantly affect the functional's computational cost in solids, and its performance for many properties [238, 249]. For example, while the HSE06 screening parameters appear nearly optimal for semiconductor bandgaps [250], they underestimate the bandgaps of large-gap insulators [218] and overestimate metals' energy bandwidths [226]. (Marques et al. [218] gives a particularly enlightening perspective on this effect, based on a relation between generalized Kohn–Sham equations with a screened hybrid functional and many-body GW calculations [251] with an effective static dielectric constant.) This has led to the exploration of several other screened hybrid forms [153, 252–257]. The "middle-range" screened hybrid HISS [152, 258] shows particular promise for surface chemistry. HISS uses a second screening function to include additional exact exchange at moderate $|\mathbf{r}-\mathbf{r}'|$. HISS accurately treats semiconductor bandgaps and lattice parameters [259], as well as some reactions on surfaces [165, 169]. Its more aggressive screening reduces its computational cost relative to HSE06 [259].

5.4 Meta-GGAs

A second route to fixing GGAs' limitations is third-rung functionals incorporating the noninteracting kinetic energy:

$$\tau(\mathbf{r}) = \frac{1}{2}\sum_i |\nabla \phi_i(\mathbf{r})|^2 = \frac{1}{2}\lim_{\mathbf{r}'\to\mathbf{r}} \nabla_{\mathbf{r}} \cdot \nabla_{\mathbf{r}'}\gamma\left(\mathbf{r},\mathbf{r}'\right), \tag{9}$$

$$E_{\mathrm{XC}}^{\mathrm{mGGA}}[\rho] = \int d^3\mathbf{r}\, e_{\mathrm{XC}}^{\mathrm{mGGA}}(\rho(\mathbf{r}), |\nabla\rho(\mathbf{r})|, \tau(\mathbf{r})). \tag{10}$$

Meta-GGAs may also use the density Laplacian, which incorporates information similar to τ [260]. Meta-GGA calculations are not much more expensive than calculations with GGAs [209, 261]. This makes meta-GGAs particularly attractive for calculations on solids and surfaces. Early meta-GGAs [262, 263] showed promise for properties such as surface energies [264] and molecular thermochemistry [261, 265]. However, their adoption was limited by the fact that they are only comparable to GGAs for lattice parameters [263] and gas-phase kinetics [266]. Modifications improving lattice parameters [267] do not improve reaction barriers [180]. This performance was somewhat disappointing, given that Eq. (9)

should contain some information about the short-range nonlocal one-particle density matrix of Eq. (6), which clearly improves hybrid functionals' performance.

A breakthrough came with the demonstration that the M06-L meta-GGA containing 37 empirical parameters can treat many properties, from lattice parameters to molecular thermochemistry to reaction barriers, with accuracy approaching hybrid functionals [268, 269]. Reverse-engineering M06-L [270] showed that part of its success comes from the inclusion of $t^{-1} = \tau/\tau_{\mathrm{HEG}}$. Here $\tau_{\mathrm{HEG}} = (3/10)(6\pi^2)^{2/3}\rho^{5/3}$ equals τ in the HEG. t^{-1} can differentiate covalent vs non-covalent interactions [270]. The success of M06-L motivated subsequent development of minimally empirical meta-GGAs based on $\alpha = (\tau - \tau_{\mathrm{W}})/\tau_{\mathrm{HEG}}$, where $\tau_{\mathrm{W}} = |\nabla\rho|^2/(8\rho) \leq \tau$, equals τ in one-electron systems [271–273]. Viewed from this perspective, M06-L becomes a meta-GGA form fit to the exact functional (which would presumably give zero error in the fitting set), whose fitting coefficients revealed meta-GGAs' previously unrecognized possibilities. Other empirical meta-GGAs have also been explored [180, 274]. These new meta-GGAs are designed in part to overcome the oscillatory behavior of M06-L [275].

6 Beyond the GGA for Surface Chemistry

The methods introduced in Sect. 5 have begun to be applied to chemistry on periodic slab model surfaces. Results to date indicate that these new methods have a great deal of potential, and point to some remaining limitations which motivate further development.

6.1 Recent Applications

One important series of studies applies the M06-L meta-GGA to molecule-surface adsorption. Hammer and coworkers showed that the M06-L meta-GGA accurately treats "medium-range" noncovalent interactions for adsorbates on graphene [270, 276, 277], despite its lack of true long-range correlation [278]. The authors have applied M06-L in subsequent studies of hydrogenation [279] and CO intercalation [280] of supported graphene, and of RS-Au-SR "staple" motifs [281] in alkanethiol monolayers on Au(111) [282].

Another important milestone concerns treatments of CO on noble metal surfaces [132]. The HSE03 screened hybrid and the M06-L and revTPSS meta-GGAs all improve the binding site preference. The meta-GGAs correctly predict that CO preferentially adsorbs atop a single Pt atom on Pt(111), along with encouraging accuracy for lattice constants, surface formation energies, and adsorption energies [283, 284]. HSE03 provides the correct site preference for CO on Cu(111) and Rh(111) surfaces. While it still fails for Pt(111), it reduces the top-fcc energy difference relative to PBE [231]. HSE03 shows similar trends for CO adsorption on the terraces of stepped Rh(553) [59].

A third application is to adsorbates and defects on metal oxide surfaces. These studies build upon screened hybrids' successes for modeling electrons localized in bulk defects [246, 285, 286]. HSE06 and the B3LYP global hybrid were used to analyze Au adatoms on ceria defects [172], a system where GGAs' over-delocalization leads to qualitatively incorrect results [213, 287]. HSE was used to check PBE + U calculations on ceria-supported vanadia catalysts [288], to confirm conclusions about the reactivity of oxygen vacancies on titania surfaces [289], and to check the spin polarization of graphite surface defects [290]. Pacchioni [291] reviews some other relevant studies.

There have been relatively few applications of meta-GGAs and screened hybrids to reaction barriers of molecules on surfaces. However, results to date suggest that these functionals' improvements for gas-phase barriers carry over to surfaces. Unlike the PBE and RPBE GGAs [162], the HSE06 screened hybrid and PBE0 global hybrid predict a substantial barrier to O_2 dissociation on Al(111) slabs [163]. (As discussed above, this failure of GGAs was previously attributed entirely to spin selection rules for triplet O_2 dissociation [162].) M06-L predicts reasonable binding energies for molecules on zeolite catalysts [83], and has been applied to heterogeneous catalysis by zeolites and metal-oxide frameworks [292, 293]. We showed that the HSE06 and HISS screened hybrids, and the M06-L meta-GGA, improved upon GGAs' underestimate of the dissociation barrier for ammonia dissociation on a cluster model of Si(100). Similar trends were seen for calculations on Si slabs [165]. We also showed that HSE06, HISS, and M06-L improve GGAs' underestimated diffusion barriers for adatoms on graphene [169] and H_2 dissociation on gold and silver clusters [160]. Interestingly, the TPSS meta-GGA increases the too-low PBE barriers for H_2 dissociation on reconstructed Si(001) surfaces, despite the two functionals' similarity for gas-phase barriers [266].

6.2 Limitations

Some studies have identified limitations of existing beyond-GGA functionals for surface chemistry. Lousada et al. [164] shows that, similar to GGAs, M06-L predicts a qualitatively incorrect barrierless dissociation of H_2O_2 on metal oxides. Valero et al. [294, 295] shows that M06-L is problematic for the frequency shifts of CO and NO on nickel and magnesium oxides. These errors are mitigated by global hybrids [294, 295]. The M06-L and TPSS meta-GGAs do not improve upon the dispersion-corrected B97-D GGA for the aforementioned problem of methanol oxidation over Au_8^-, giving mean unsigned errors in reaction barrier heights of 10.1, 9.2, and 7.4 kcal mol^{-1}, respectively [31]. However, the B3LYP and M06 [269] global hybrids improve upon B97-D, with errors of 3.6 and 3.9 kcal mol^{-1}. HSE06's overestimated metal bandwidths [226] appear to contribute to its aforementioned problems for CO on Pt(111) [231]. The B3LYP global hybrid has other

problems for metals, which arise because its GGA for correlation [69] does not recover the correct HEG behavior [296].

6.3 Systematic Trends

Our recent extension [169] of diffusion Monte Carlo studies on adatom adsorption and diffusion over graphene [34] provides a systematic illustration of how screened exchange affects the Procrustean dilemma [62] faced by GGAs for surface chemistry. Part of that study considered systematic modification of the PBE GGA by both rescaling of the exchange enhancement factor ($F_X = \beta F_X^{PBE}$, see (3)), and admixture of a fraction α of screened exact exchange. (Put another way, changing β is similar to specific reaction parameter GGAs used for surface chemistry [181, 182]. Changing α is similar to the original specific reaction parameter global hybrids [183]). Figure 4 illustrates how changing β and α affect representative surface and molecule properties. The left panel shows calculated adsorption energies and diffusion barriers for O atom on graphene, compared to the diffusion Monte Carlo results of Hsing et al. [34]. The right panel shows errors in standard sets of gas-phase molecular thermochemistry and kinetics [297]. Computational details are in Barone et al. [169].

Figure 4 shows that GGA rescaling β simultaneously changes both adsorption energies and reaction barriers, and that *no* value of β can treat both properties. Figure 3 of Barone et al. [169] shows that a simple dispersion correction increased the GGA chemisorption energies, but did not affect reaction barriers. This is consistent with the results of Fig. 2 and with the limitations of empirical GGAs discussed in Sect. 4. In contrast, screened exchange admixture α increases both

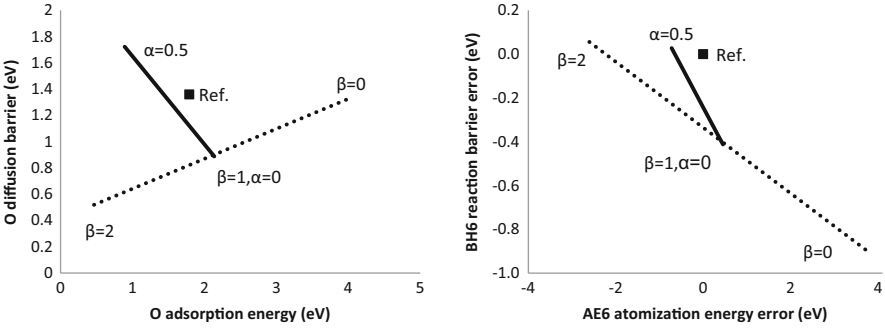

Fig. 4 Systematic variations in GGA enhancement factor $F_X = \beta F_X^{PBE}$ (*dotted lines*) and screened exchange admixture α (*solid lines*). $\beta = 1$, $\alpha = 0$ is the PBE GGA, $\beta = 1$, $\alpha = 0.25$ is the HSE06 screened hybrid. *Left*: Diffusion barrier vs adsorption energy for O on graphene. *Right*: Mean signed errors in gas-phase BH6 [297] kinetics vs AE6 thermochemistry. "Ref." are diffusion Monte Carlo from Ren et al. [34] (*left*) and zero mean signed error (*right*). Adapted with permission from Barone et al. [169]. Copyright 2013 American Chemical Society

surface diffusion barriers and molecule reaction barriers, while maintaining reasonable thermochemistry and atomization energies. The results suggest that screened hybrids have the potential to improve reaction barriers on surfaces, just as global hybrids improve gas-phase reaction barriers.

7 New Frontiers

Meta-GGAs and screened hybrids are not yet standard methods for simulating heterogeneous catalysis or surface chemistry. Additional work is needed to understand better their strengths and limitations, and to develop more accurate extensions. This section briefly reviews selected recent work along those lines, focusing on results from the author and his collaborators.

7.1 Dispersion-Corrected and Empirical Screened Hybrids

Barone et al. [169] suggests that GGAs' limitations for dispersion interactions and reaction barriers are largely orthogonal. Dispersion-corrected screened hybrids could in principle combine the aforementioned successes of dispersion corrections for adsorption energies and hybrid exchange for reaction barriers. A dispersion-corrected screened hybrid was recently benchmarked for rare-gas solids [255], and applied to C–H bond cleavage in crystalline polyethylene [298] and Au adatom adsorption on defective CeO_2(111) [172] mimicking ceria-supported gold catalysts [299]. Dispersion-corrected PBE and HSE calculations gave similar barriers to tetrachloropyrazine chemisorption on Pt(111) [300]. Dispersion-corrected global hybrids have also been applied to some molecular crystals [301], crystalline polymers [302], and surface chemistry [303].

It is interesting to consider whether empirical functional forms [173, 174, 179, 180] could benefit from screened exchange admixture. Perverati and Truhlar [257] proposed screened hybrids built upon the parameterizations of [179, 180]. These functionals improve upon HSE06 for gas-phase reaction barriers and some lattice constants [257]. They show modest promise for binding and relative energies of water clusters, properties which appear to be improved by dispersion corrections [304]. However, they have not yet been extensively tested for surface chemistry.

7.2 Rung 3.5 Functionals

We have proposed a new class of approximate functionals constructed to be intermediate between third-rung meta-GGAs and fourth-rung screened hybrids.

Rung 3.5 functionals replace one of the one-particle density matrices in (4) with a GGA model density matrix γ_{GGA}:

$$E_X^{\Pi}[\rho] = -\frac{1}{2}\int d^3\mathbf{r}\int d^3\mathbf{r}'\,\frac{\gamma(\mathbf{r},\mathbf{r}')\gamma_{GGA}\left(\rho(\mathbf{r}),\nabla\rho(\mathbf{r}),\mathbf{r}-\mathbf{r}'\right)}{|\mathbf{r}-\mathbf{r}'|}. \tag{11}$$

The integrand of (11) is symmetrized in $\mathbf{r}, \mathbf{r}'$ before use. The GGA model density matrix is implicit in the construction of the GGA exchange hole of Eq. (8):

$$h_X^{GGA}\left(\rho(\mathbf{r}),\nabla\rho(\mathbf{r}),|\mathbf{r}-\mathbf{r}'|\right) = -\frac{1}{2}\rho^{-1}(\mathbf{r})\left\langle\left|\gamma_{GGA}\left(\rho(\mathbf{r}),\nabla\rho(\mathbf{r}),\mathbf{r}-\mathbf{r}'\right)\right|^2\right\rangle_{\Omega}, \tag{12}$$

where $\langle\ldots\rangle_{\Omega}$ denotes angle averaging. Most existing exchange hole models treat the angle- and system-averaged hole [240, 241], while γ_{GGA} is explicitly not angle averaged [305]. γ_{GGA}, similar to h_X^{GGA}, decays rapidly in $|\mathbf{r}-\mathbf{r}'|$ by construction, aiding evaluation of Eq. (11) in metals. (Recall from Sect. 5.1 that this localization is central to the GGA "exchange" functionals' model of nondynamical correlation.) γ_{GGA} also tunes the amount of nonlocal information incorporated at each point, potentially providing a route to simultaneously treating several of the regions in Fig. 3. (Note that Eq. (11) cannot include 100% long-range exact exchange, and is not exact for one-electron regions.) Rung 3.5 functionals thus have the potential to address all three limitations of exact exchange admixture discussed in Sect. 5.1. Janesko [306] reviews our applications of Rung 3.5 functionals. Benchmarks for molecular thermochemistry and kinetics show that they can provide accuracy intermediate between standard GGAs and screened hybrids.

Table 1 presents previously unpublished results applying the Rung 3.5 functional *Π* 1PBE [305] to ammonia dissociation on Si(100). *Π* 1PBE admixes 25% of Eq. (11) to the PBE GGA, using a model density matrix γ_{PBE} constructed to reproduce the PBE exchange enhancement factor. Calculations use a small cluster model (nine Si atoms) from Sniatynsky et al. [165]. The Rung 3.5 reaction barrier is between the third-rung TPSS meta-GGA and the fourth-rung HSE06 screened

Table 1 Adsorption and dissociation of NH_3 on Si (100)

Method	ΔE_{ads}	$\Delta E^{\ddagger}$	ΔE_{rxn}
PBE	−1.01	0.67	−0.99
TPSS	−0.97	0.71	−1.15
Π 1PBE	−1.11	0.74	−1.03
HSE06	−1.13	0.80	−1.11
ref	−1.08	0.86	−1.19

Calculated Si–NH_3 adsorption energy ΔE_{ads}, and dissociation barrier $\Delta E^{\ddagger}$ and reaction energy ΔE_{rxn} (eV) for adsorbed NH_2–H bond dissociation. Results for NH_3 adsorbed to a cluster model for the Si(001) surface. DFT calculations use the 6-311++G (2d,2p) basis set, other computational details and "ref" complete-basis-set-extrapolated CCSD(T) benchmarks are in Sniatynsky et al. [165]

hybrid, indicating that the functional lives up to its name. (Results in Table 1 differ by ~0.02 eV from Sniatynsky et al. [165] because of a different basis set.) We are currently exploring more extensive applications of Rung 3.5 functionals to surface chemistry.

8 Conclusions

The successes of GGAs for surface chemistry are particularly remarkable, given their underlying limitations. Density functional approximations beyond the GGA, largely developed in the computational chemistry community, show promise for ameliorating these limitations in simulations of surface chemistry. Recent calculations illustrate these new methods' potential and point to remaining issues. It is hoped that these promising preliminary results motivate density functional developers to consider further the applications to surfaces, and motivate surface scientists to test beyond-GGA approximations on new systems. More accurate, computationally tractable methods including beyond-GGA DFT will help build upon GGAs' successes for surface chemistry.

Acknowledgements This work was supported by the Qatar National Research Foundation through the National Priorities Research Program (NPRP Grant No. 09-143-1-022), and by the Department of Chemistry at Texas Christian University.

References

1. Ertl G (2009) Reactions at solid surfaces. Wiley, Hoboken
2. Kneipp J, Kneipp H, Kneipp K (2008) Chem Rev 37:1052
3. Manthiram A, Murugan AV, Sarkar A, Muraliganth T (2008) Energy Environ Sci 1:621
4. Yazev O (2013) Acc Chem Res 46:2319
5. The Nobel Prize in Chemistry 2007. Nobelprize.org. Nobel Media AB 2013. Web 8 Dec 2013
6. Dry ME (2002) Catal Today 71:227
7. Schulz H (1999) Appl Catal Gen 186:3
8. Galvis HMT, Koeken AC, Bitter JH, Davidian T, Ruitenbeek M, Dugulan AI, de Jong KP (2013) J Catal 303:22
9. Mitchell WJ, Wang Y, Xie J, and Weinberg WH (1993) J Am Chem Soc 115:4381
10. Heiz U, Schneider WD (2000) J Phys D Appl Phys 33:R85
11. Zhang S, Nguyen L, Zhu Y, Zhan S, Tsung CKF, Tao FF (2013) Acc Chem Res 46:1731
12. Vang RT, Lauritsen JV, Lægsgaard E, Bensebacher F (2008) Chem Soc Rev 37:2191
13. Maitlis PM (2004) J Organomet Chem 689:4366
14. Neurock M, van Santen RA (2006) Molecular heterogeneous catalysis: a conceptual and computational approach. Wiley-VCH Verlag GmbH & Co. KGaA, Weinham
15. Schatz GC, Van Duyne RP (2002) In: Chalmers JM, Griffiths PR (eds) Handbook of vibrational spectroscopy. Wiley, New York
16. Zhao LL, Jensen L, Schatz GC (2006) J Am Chem Soc 128:2911
17. Son YW, Cohen ML, Louie SG (2006) Nature 444:347

18. Ovesen CV, Clausen BS, Hammershøi BS, Steffensen G, Askgaard T, Chorkendorff I, Nørskov JK, Rasmussen PB, Stoltze P, Taylor P (1996) J Catal 158:170
19. Callaghan C, Fishtik I, Datta R (2002) Worchester Polytechnic Institute, Fuel Chemistry Division Preprints
20. Grabow LC, Gokhale AA, Evans ST, Dumesic JA, Mavrikakis M (2008) J Phys Chem C 112:4608
21. Mirwald JR, Inderwildi OR (2012) Phys Chem Chem Phys 14:7028
22. Lanzani G, Martinazzo R, Materzanini G, Pino I, Tantardini GF (2007) Theor Chem Acc 117:805
23. Czekaj I, Wambach J, Kröcher O (2009) Int J Mol Sci 10:4310
24. Huang P, Carter EA (2008) Annu Rev Phys Chem 59:261
25. Bauschlicher CW Jr (1994) J Chem Phys 101:3250
26. Filippi C, Healy SB, Kratzer P, Pehlke E, Scheffler M (2002) Phys Rev Lett 89:166102
27. Szabo A, Ostlund NS (1989) Modern quantum chemistry: introduction to advanced electronic structure theory. Dover Publications Inc., Mineola, New York
28. de Jong GT, Bickelhaupt FM (2006) J Chem Theory Comput 2:322
29. Njegic B, Gordon MS (2008) J Chem Phys 129:124705
30. Wang Y, Qian HJ, Morokuma K, Irle S (2012) J Phys Chem A 116:7154
31. Hansen JA, Ehara M, Piecuch P (2013) J Phys Chem A 117:10416
32. Pozzo M, Alfè D (2008) Phys Rev B 78:245313
33. Kanai Y, Takeuchi N (2009) J Chem Phys 131:214708
34. Hsing CR, Wei CM, Chou MY (2012) J Phys Condens Matter 24:395002
35. Hoggan PE (2013) Int J Quant Chem 113:277
36. Ren X, Rinke P, Scheffler M (2009) Phys Rev B 80:045402
37. Göltl F, Grüneis A, Bučko T, Hafner J (2012) J Chem Phys 137:114111
38. Mittendorfer F, Garhofer A, Redinger J, Klimeš J, Harl J, Kresse G (2011) Phys Rev B 84:201401
39. Ren X, Rinke P, Joas C, Scheffler M (2012) J Mater Sci 47:7447
40. Kim HJ, Tkatchenko A, Cho JH, Scheffler M (2012) Phys Rev B 85:041403(R)
41. Karlický F, Lazar P, Dubecký M, Otyepka M (2013) J Chem Theory Comput 9:3670
42. Olsen T, Thygesen KS (2013) Phys Rev B 87:075111
43. Hayashi K, Sato S, Bai S, Higuchi Y, Ozawa N, Shimazaki T, Adachi J, Martin JM, Kubo M (2012) Faraday Discuss 156:137
44. Hohenberg P, Kohn W (1964) Phys Rev B136:864
45. Kohn W, Sham L (1965) Phys Rev 140:A1133
46. ISI Web of Science. Accessed 17 Dec 2013
47. Burke K (2012) J Chem Phys 136:150901
48. Bartlett RJ, Schweigert IV, Lotrich VF (2006) J Mol Struct 771:1
49. Perdew JP, Schmidt K (2001) In: Van Doren V, Van Alsenoy C, Geerlings P (eds) Density functional theory and its application to materials. American Institute of Physics, Melville, pp 1–20
50. Perdew JP (1986) Phys Rev A 33:8822
51. Vosko SH, Wilk L, Nusair M (1980) Can J Phys 58(8):1200
52. Gell-Mann M, Brueckner KA (1957) Phys Rev 106:364
53. Ceperley DM, Alder BJ (1980) Phys Rev Lett 45:566
54. Burke K, Cruz FG, Lam KC (1998) J Chem Phys 109(19):8161
55. Perdew JP, Burke K, Ernzerhof M (1996) Phys Rev Lett 77:3865, 78:1396(E) (1997)
56. Becke AD (1993) J Chem Phys 98(2):1372
57. Slater JC (1951) Phys Rev 81:385
58. Janthon P, Kozlov SM, Viñes F, Limtrakul J, Illas F (2013) J Chem Theory Comput 9:1631
59. Stroppa A, Kresse G (2008) New J Phys 10:063020
60. Schimka L, Harl J, Stroppa A, Grüneis A, Marsman M, Mittendorfer F, Kresse G (2010) Nat Mater 9:741

61. Goerigk L, Grimme S (2011) Phys Chem Chem Phys 13:6670
62. Perdew JP, Ruzsinszky A, Csonka GA, Vydrov OA, Scuseria GE, Constantin LI, Zhou X, Burke K (2008) Phys Rev Lett 100:136406
63. Armiento R, Mattsson AE (2005) Phys Rev B 72:085108
64. Wu Z, Cohen RE (2006) Phys Rev B 73:235116
65. Tran F, Lasowski R, Blaha P, Schwarz K (2007) Phys Rev B 75:115131
66. Zhang Y, Yang W (1998) Phys Rev Lett 80:890
67. Hammer B, Hansen LB, Nørskov JK (1999) Phys Rev B 59:7413
68. Becke AD (1988) Phys Rev A 38:3098
69. Lee C, Yang W, Parr RG (1988) Phys Rev B 37:785
70. Becke AD (1992) J Chem Phys 96:2155
71. Hamprecht FA, Cohen AJ, Tozer DJ, Handy NC (1998) J Chem Phys 109:6264
72. Perdew JP (1991) In: Ziesche P, Eschrig H (eds) Electronic structure of solids'91. Akademie Verlag, Berlin
73. Patton DC, Pederson MR (1997) Phys Rev A 56:R2495
74. Grimme S (2011) WIREs Comput Mol Sci 1:211
75. Johnson ER, Mackie ID, DiLabio GA (2009) J Phys Organ Chem 22:1127
76. Klimes J, Michaelides A (2012) J Chem Phys 137:120901
77. Ramalho JAPP, Gomes JRB, Illas F (2013) RSC Adv 3:13085
78. Thrower JD, Friis EE, Skov AL, Nilsson L, Andersen M, Ferrighi L, Jrgensen B, Baouche S, Balog R, Hammer B, Hornekr L (2013) J Phys Chem C 117(26):13520
79. Romaner L, Nabok D, Puschnig P, Zojer E, Ambrosch-Draxl C (2009) New J Phys 11:053010
80. Ruiz VG, Liu W, Zojer E, Scheffler M, Tkatchenko A (2012) Phys Rev Lett 108:146103
81. Londero E, Karlson EK, Landahl M, Ostrovskii D, Rydberg JD, Schröder E (2012) J Phys Condens Matter 24(42):424212
82. Rakow JR, Tüllmann S, Holthausen MC (2009) J Phys Chem A 113:12035
83. Zhao Y, Truhlar DG (2008) J Phys Chem C 112:6860
84. Gomes J, Zimmerman PM, Head-Gordon M, Bell AT (2012) J Phys Chem C 116:15406
85. Goerigk L, Grimme S (2010) J Chem Theory Comput 6:107
86. Zhao Y, Lynch BJ, Truhlar DG (2004) J Phys Chem A 108:2715
87. Zhao Y, Gonzáles-García N, Truhlar DG (2005) J Phys Chem A 109:2012, 110:4942 (E) (2006)
88. Gerber IC, Ángyán JG (2007) J Chem Phys 126:044103
89. Schwabe T, Grimme S (2007) Phys Chem Chem Phys 9:3397
90. Benighaus T, DiStasio RA Jr, Lochan RC, Chai JD, Head-Gordon M (2008) J Phys Chem A 112:2702
91. Chai JD, Head-Gordon M (2008) Phys Chem Chem Phys 10:6615
92. Lin YS, Li GD, Mao SP, Chai JD (2012) J Chem Theory Comput. dx.doi.org/10.1021/ct300715s
93. Svelle S, Tuma C, Rozanska X, Kerber T, Sauer J (2009) J Am Chem Soc 131(2):816
94. Hafner J (2008) J Comput Chem 29:2044
95. Greeley J, Nørskov JK, Mavrikakis M (2002) Annu Rev Phys Chem 53:319
96. Nørskov JK, Abild-Pedersen F, Studt F, Bligaard T (2011) Proc Natl Acad Sci USA 108:937
97. Hod O, Peralta JE, Scuseria GE (2007) Phys Rev B 76:233401
98. Chen Z, Lu YM, Rooks MJ, Avouris P (2007) Physica E 40:228
99. Han MY, Özyilmaz B, Zhang Y, Kim P (2007) Phys Rev Lett 98:206805
100. Kozlov SM, Viñes F, Görling A (2011) Adv Mater 23:2638
101. Balog R, Jrgensen B, Nilsson L, Andersen M, Rienks E, Bianchi M, Fanetti M, Lgs-gaard E, Baraldi A, Lizzit S, Sljivancanin Z, Besenbacher F, Hammer B, Pedersen TG, Hofmann P, Hornekr L (2010) Nat Mater 9:315
102. Lopez-Bezanilla A, Huang J, Terrones H, Sumpter BG (2011) Nano Lett 11:3267
103. Miotto R, Srivastava GP, Ferraz AC (1998) Phys Rev B 58:7944
104. Lee SH, Kang MH (1998) Phys Rev B 58:4903

105. Chung ON, Kim H, Chung S, Koo JY (2006) Phys Rev B 73:033303
106. Bowler DR, Owen JHG (2007) Phys Rev B 75:155310
107. Owen JHG (2009) J Phys Condens Matter 21:44301
108. Honkala K, Hellman A, Remediakis IN, Logadottir A, Carlsson A, Dahl S, Christiansen CH, Nørskov JK (2005) Science 307:555
109. Dahl S, Logadottir A, Egeberg RC, Larsen JH, Chorkendorff I, Törnqvist E, Nørskov JK (1999) Phys Rev Lett 83:1814
110. Ciobica IM, Van Santen RA (2003) J Phys Chem B 107:3808
111. Inderwildi OR, Jenkins SJ, King DA (2008) J Phys Chem C 112:1305
112. Andersson M, Abild-Pedersen F, Remediakis I, Bligaard T, Jones G, Engæk J, Lytken O, Horch S, Nielsen J, Sehested J, Rostrup-Nielsen J, Nørskov J, Chorkendorff I (2008) J Catal 255:6
113. Inderwildi OR, Jenkins SJ, King DA (2008) Angew Chem Int Ed 47:5253
114. Ojeda M, Nabar R, Nilekar AU, Ishikawa A, Mavrikakis M, Iglesia E (2010) J Catal 272:287
115. Shetty S, Jansen PJ, van Santen RA (2009) J Am Chem Soc 131:12874
116. Liu ZP, Hu P (2002) J Am Chem Soc 124:11568
117. Huo CF, Wu BS, Gao P, Li YYYW, Jiao H (2011) Angew Chem Int Ed 50:7403
118. Bengaard H, Nørskov J, Sehested J, Clausen B, Nielsen L, Molenbroek A, Rostrup-Nielsen J (2002) J Catal 209(2):365
119. Curulla-Ferre D, Govender A, Bromfield TC, Niemantsverdriet JWH (2006) J Phys Chem B 110:13897
120. Ge Q, Neurock M (2006) J Phys Chem B 110:15368
121. Cheng J, Hu P, Ellis P, French S, Kelly G, Lok CM (2010) Topics Catal 53:326
122. van Santen RA, Ghouri MM, Shetty S, Hensen EMH (2011) Catal Sci Technol 1:891
123. Alfonso DR (2013) J Phys Chem C 117:20562
124. Newsome DS (1980) Catal Rev Sci Eng 21:275
125. Gokhale AA, Dumesic JA, Mavrikakis M (2008) J Am Chem Soc 130:1402
126. Grabow LC, Mavrikakis M (2011) ACS Catal 1:365
127. Sanchez A, Abbet S, Heitz U, Scheider WD, Häkkinen H, Barnett RN, Landman U (1999) J Phys Chem A 103:9573
128. Yoon B, Häkkinen H, Landman U, Wörz AS, Antonetti JM, Abbet S, Judai K, Heitz U (2005) Science 307:403
129. Janssens TVW, Clausen BS, Hvolbk B, Falsig H, Christensen CH, Bligaard T, Nrskov JK (2007) Topics Catal 44:15
130. Boronat M, Concepción P, Corma A (2009) J Phys Chem C 113:16772
131. Zhang C, Michaelides A, Jenkins ST (2011) Phys Chem Chem Phys 13:22
132. Feibelman PJ, Hammer B, Nørskov JK, Wagner F, Scheffler M, Stumpf R, Watwe R, Dumesic J (2001) J Phys Chem B 105:4018
133. Hammer B, Morikawa Y, Nørskov JK (1996) Phys Rev Lett 76:2141
134. Abild-Pedersen F, Greeley J, Studt F, Rossmeisl J, Munter TR, Moses PG, Skulason E, Bligaard T, Norskov JK (2007) Phys Rev Lett 99:016105
135. Luengnaruemitchai A, Osuwan S, Gulari E (2003) Catal Commun 4:215
136. Schumachera N, Boisena A, Dahl S, Gokhalec AA, Kandoic S, Grabowc L, Dumesicc J, Mavrikakis M, Chorkendorff I (2005) J Catal 229:265
137. Bligaard T, Nørskov JK, Dahl S, Matthiesen J, Christensen CH, Sehested J (2004) J Catal 224:206
138. Cheng J, Hu P (2008) J Am Chem Soc 130:10868
139. Andersson MP, Bligaard T, Kustov A, Larsen KE, Greeley J, Johannessen T, Christensen CH, Nørskov JK (2006) J Catal 239:501
140. Sehested J, Larsen KE, Kustov AL, Frey AM, Johannessen T, Bligaard T, Andersson MP, Nørskov JK, Christensen CH (2007) Topics Catal 45:9
141. Studt F, Abild-Pedersen F, Bligaard T, Sørensen RJ, Christiansen CH, Nørskov JK (2009) Science 320:1320

142. Greeley J, Mavrikakis M (2004) Nat Mater 3:810
143. Nørskov JK, Bligaard T, Rossmeisl J, Christiansen CH (2009) Nat Chem 1:37
144. Mori-Sánchez P, Cohen AJ, Yang W (2006) J Chem Phys 125:201102
145. Perdew JP, Ruzsinszky A, Constantin LA, Sun J, Csonka GI (2009) J Chem Theory Comput 5:902
146. Csonka GI, Perdew JP, Ruzsinszky A (2010) J Chem Theory Comput 6(12):3688
147. Deng L, Branchadell V, Ziegler T (1994) J Am Chem Soc 116:10645
148. Andersson S, Grüning M (2004) J Phys Chem A 108:7621
149. Riley KE, Op't Holt BT, Merz KE Jr (2007) J Chem Theory Comput 3:407
150. Zheng J, Zhao Y, Truhlar DG (2009) J Chem Theory Comput 5:808
151. Yang K, Zheng J, Zhao Y, Truhlar DG (2010) J Chem Phys 132:164117
152. Henderson TM, Izmaylov AF, Scuseria GE, Savin A (2008) J Chem Theory Comput 4:1254
153. Janesko BG, Scuseria GE (2008) J Chem Phys 129:124110
154. Mangiatordi GF, Brémond E, Adamo C (2012) J Chem Theory Comput 8:3082
155. Nachtigall P, Jordan KD, Smith A, Jónsson H (1996) J Chem Phys 104:148
156. Dürr M, Raschke MB, Pehlke E, Höfer U (2001) Phys Rev Lett 86:123
157. de Jong GT, Bickelhaupt FM (2005) J Phys Chem A 109:9685
158. de Jong GT, Geerke DP, Diefenbach A, Bickelhaupt FM (2005) Chem Phys 313:261
159. de Jong GT, Geerke DP, Diffenbach A, Solá M, Bickelhaupt FM (2005) J Comput Chem 26:1007
160. Moncho S, Brothers EN, Janesko BG (2013) J Phys Chem C 117:7487
161. Livshits E, Baer R, Kosloff R (2009) J Phys Chem A 113:7521
162. Behler J, Delley B, Lorenz S, Reuter K, Scheffler M (2005) Phys Rev Lett 94:036104
163. Liu HR, Xiang H, Gong XG (2011) J Chem Phys 135:214702
164. Lousada CM, Johansson AJ, Brinck T, Jonsson M (2013) Phys Chem Chem Phys 15:5539
165. Sniatynsky R, Janesko BG, El-Mellouhi F, Brothers EN (2012) J Phys Chem C 116:26396
166. Hossain MZ, Yamashita Y, Mukai K, Yoshinobu J (2003) Phys Rev B 68:235322
167. Smedarchina ZK, Zgierski MZ (2003) Int J Mol Sci 4:445
168. Uthaisar C, Barone V (2010) Nano Lett 10:2838
169. Barone V, Brothers EN, Janesko BG (2013) J Chem Theory Comput 9:4853
170. Lopez N, Illas F, Rösch N, Pacchioni G (1999) J Chem Phys 110:4873
171. Di Valentin C, Pacchioni G, Selloni A (2006) Phys Rev Lett 97:166803
172. Pan Y, Nilius N, Freund HJ, Paier J, Penschke C, Sauer J (2013) Phys Rev Lett 111:206101
173. Becke AD (1997) J Chem Phys 107:8554
174. Wellendorff J, Lundgaard KT, Møgelhøj A, Petzold V, Landis DD, Nørskov JK, Bligaard T, Jacobsen KW (2012) Phys Rev B 85:235149
175. Rajasekaran S, Abild-Pedersen F, Ogasawara H, Nilsson A, Kaya S (2013) Phys Rev Lett 111:085503
176. Brogaard RY, Weckhuysen BM, Nørskov JK (2013) J Catal 300:235
177. Studt F, Abild-Pedersen F, Varley JB, Nørskov JK (2013) Catal Lett 143:71
178. Peverati R, Zhao Y, Truhlar DG (2011) J Phys Chem Lett 2:1991
179. Perverati R, Truhlar DG (2012) J Chem Theory Comput 8:2310
180. Perverati R, Truhlar DG (2012) Phys Chem Chem Phys 14:13171
181. Díaz C, Pijper E, Olsen RA, Busnengo HF, Auerbach DJ, Kroes GJ (2009) Science 326:832
182. Kroes GJ (2012) Phys Chem Chem Phys 14:14966
183. Chuang YY, Radhakrishnan ML, Fast PL, Cramer CJ, Truhlar DG (1999) J Phys Chem A 103:4893
184. Yang W (1998) J Chem Phys 109:10107
185. Kim MC, Sim E, Burke K (2013) Phys Rev Lett 111:073003
186. Vydrov OA, Scuseria GE, Perdew JP, Ruzsinszky A, Csonka GI (2006) J Chem Phys 124:094108
187. Wu Q, Kaduk B, van Voorhis T (2008) J Chem Phys 130:034109
188. Cremer D (2001) Mol Phys 99(23):1899

189. Perdew JP, Staroverov VN, Tao J, Scuseria GE (2008) Phys Rev A 78:052513
190. Yang W, Zhang Y, Ayers PW (2000) Phys Rev Lett 84:5172
191. Zhang Y, Yang W (1998) J Chem Phys 109(7):2604
192. Ruzsinszky A, Perdew JP, Csonka GI, Vydrov OA, Scuseria GE (2006) J Chem Phys 125:194112
193. Mori-Sánchez P, Cohen AJ, Yang W (2008) Phys Rev Lett 100:146401
194. Burke K, Perdew JP, Ernzerhof M (1998) J Chem Phys 109:3760
195. Garza AJ, Jimenez-Hoyos CA, Scuseria GE (2013) J Chem Phys 138:134102
196. Seidl A, Görling A, Vogl P, Majewski JA, Levy M (1996) Phys Rev B 53:3764
197. Cohen AJ, Mori-Sánchez P, Yang W (2008) Phys Rev B 77:115123
198. Yang W, Cohen AJ, Mori-Sánchez P (2012) J Chem Phys 136:204111
199. Sharp RT, Horton GK (1953) Phys Rev 90:317
200. Krieger JB, Li Y, Iafrate GJ (1992) Phys Rev A 45:101
201. Ivanov S, Hirata S, Bartlett RJ (1999) Phys Rev Lett 83:5455
202. Staroverov VN, Scuseria GE, Davidson ER (2006) J Chem Phys 124:114103
203. Becke AD (1993) J Chem Phys 98(7):5648
204. Stephens PJ, Devlin FJ, Chabalowski CF, Frisch MJ (1994) J Phys Chem 98(45):11623
205. Lynch BJ, Fast PL, Harris M, Truhlar DG (2000) J Phys Chem A 104(21):4811
206. Stoll H, Savin A (1985) In: Dreizler R, da Providencia J (eds) Density functional methods in physics. Plenum, New York, p 177
207. Savin A (1996) In: Seminario JM (ed) Recent developments and applications of modern density functional theory. Elsevier, Amsterdam, p 327
208. Leininger T, Stoll H, Werner HJ, Savin A (1997) Chem Phys Lett 275:151
209. Furche F, Perdew JP (2006) J Chem Phys 124:044103
210. Schultz NE, Zhao Y, Truhlar DG (2005) J Phys Chem A 109:11127
211. Hafner J (2008) Montash Chem 139:373
212. Anisimov VI, Zaanen J, Andersen OK (1991) Phys Rev B 44:943
213. Loschen C, Carrasco J, Neyman KM, Illas F (2007) Phys Rev B 75(3):035115
214. Baer R, Neuhauser D (2005) Phys Rev Lett 94:043002
215. Livshits E, Baer R (2007) Phys Chem Chem Phys 9:2932
216. Stein T, Kronik L, Baer R (2009) J Am Chem Soc 131:2818
217. Odashima MM, Capelle K (2009) Phys Rev A 79:062515
218. Marques MAL, Vidal J, Oliveria MJT, Reining L, Botti S (2011) Phys Rev B 83:035119
219. Stein T, Eisenberg H, Kronik L, Baer R (2010) Phys Rev Lett 105:266802
220. Jaramillo J, Scuseria GE, Ernzerhof M (2003) J Chem Phys 118(3):1068
221. Arbuznikov AV, Kaupp M (2011) Int J Quant Chem 111:2625
222. Haunschild R, Odashima MM, Scuseria GE, Perdew JP, Capelle K (2012) J Chem Phys 136:184102
223. Becke AD (2003) J Chem Phys 119(6):2972
224. Becke AD (2005) J Chem Phys 122:064101
225. Arbuznikov AV, Kaupp M (2012) J Chem Phys 136:014111
226. Paier J, Marsman M, Hummer K, Kresse G, Gerber IC, Ángyán JA (2006) J Chem Phys 124:154709
227. Gygi F, Baldereschi A (1986) Phys Rev B 34:4405
228. Broqvist P, Alkauskas A, Pasquarello A (2009) Phys Rev B 80:085114
229. Zecca L, Gori-Giorgi P, Moroni S, Bachelet GB (2004) Phys Rev B 70:205127
230. Monkhorst HJ (1979) Phys Rev B 20:1504
231. Stroppa A, Termentzidis K, Paier J, Kresse G, Hafner J (2007) Phys Rev B 76:195440
232. Gil A, Clotet A, Ricart JM, Kresse G, Garciá-Hernández M, Rösch N, Sautet P (2003) Surf Sci 530:71
233. Doll K (2004) Surf Sci 573:464
234. Bylander DM, Kleinman L (1990) Phys Rev B 41:7868
235. Heyd J, Scuseria GE, Ernzerhof M (2003) J Chem Phys 118(18):8207, 124:219906 (2006)

236. Toulouse J, Colonna F, Savin A (2004) Phys Rev A 70:062505
237. Barone V, Hod O, Peralta JE, Scuseria GE (2011) Acc Chem Res 44:269
238. Krukau AV, Vydrov OA, Izmaylov AF, Scuseria GE (2006) J Chem Phys 125:224106
239. Henderson TM, Izmaylov AF, Scalmani G, Scuseria GE (2009) J Chem Phys 131:044108
240. Ernzerhof M, Perdew JP (1998) J Chem Phys 109(9):3313
241. Henderson TM, Janesko BG, Scuseria GE (2008) J Chem Phys 128:194105
242. Heyd J, Scuseria GE (2004) J Chem Phys 120:7274
243. Frisch MJ, Trucks GW, Schlegel HB, Scuseria GE, Robb MA, Cheeseman JR, Scalmani G, Barone V, Mennucci B, Petersson GA, Nakatsuji H, Caricato M, Li X, Hratchian HP, Izmaylov AF, Bloino J, Zheng G, Sonnenberg JL, Hada M, Ehara M, Toyota K, Fukuda R, Hasegawa J, Ishida M, Nakajima T, Honda Y, Kitao O, Nakai H, Vreven T, Montgomery JA Jr, Peralta JE, Ogliaro F, Bearpark M, Heyd JJ, Brothers E, Kudin KN, Staroverov VN, Keith T, Kobayashi R, Normand J, Raghavachari K, Rendell A, Burant JC, Iyengar SS, Tomasi J, Cossi M, Rega N, Millam JM, Klene M, Knox JE, Cross JB, Bakken V, Adamo C, Jaramillo J, Gomperts R, Stratmann RE, Yazyev O, Austin AJ, Cammi R, Pomelli C, Ochterski JW, Martin RL, Morokuma K, Zakrzewski VG, Voth GA, Salvador P, Dannenberg JJ, Dapprich S, Daniels AD, Farkas O, Foresman JB, Ortiz JV, Cioslowski J, Fox DJ (2010) Gaussian 09, Revision B.01. Gaussian Inc., Wallingford
244. Kresse G, Furthmüller J (1996) Phys Rev B 54:11169
245. Marsman M, Paier J, Stroppa A, Kresse G (2008) J Phys Condens Matter 20:064201
246. Janesko BG, Henderson TM, Scuseria GE (2009) Phys Chem Chem Phys 11:443
247. Henderson TM, Janesko BG, Scuseria GE (2008) J Phys Chem A 112:12530
248. Perdew JP, Ernzerhof M, Burke K (1996) J Chem Phys 105(22):9982
249. Moussa JA, Schultz PA, Chelikowsky JR (2012) J Chem Phys 136:204117
250. Heyd J, Peralta JE, Scuseria GE, Martin RL (2005) J Chem Phys 123:174101
251. Hedin L (1965) Phys Rev 139:A796
252. Iikura H, Tsuneda T, Yanai T, Hirao K (2001) J Chem Phys 115:3540
253. Krukau AV, Scuseria GE, Perdew JP, Savin A (2008) J Chem Phys 129:124103
254. Shimka L, Harl J, Kresse G (2011) J Chem Phys 134:024116
255. Yousaf KE, Brothers EN (2010) J Chem Theory Comput 6:864
256. Song JW, Yamashita K, Hirao K (2011) J Chem Phys 135:071103
257. Perverati R, Truhlar DG (2012) Phys Chem Chem Phys 14:16187
258. Henderson TM, Izmaylov AF, Scuseria GE, Savin A (2007) J Chem Phys 127:221103
259. Lucero MJ, Henderson T, Scuseria GE (2012) J Phys Condens Matter 24:145504
260. Constantin LA, Perdew JP (2006) Phys Rev B 75:155109
261. Staroverov VN, Scuseria GE, Tao J, Perdew JP (2003) J Chem Phys 119(23):12129
262. Perdew JP, Kurth S, Zupan A, Blaha P (1999) Phys Rev Lett 82:2544, 82:5179 (1999)
263. Tao J, Perdew JP, Staroverov VN, Scuseria GE (2003) Phys Rev Lett 91:146401
264. Almeida LM, Perdew JP, Fiolhais C (2002) Phys Rev B 66:075115
265. Van Voorhis T, Scuseria GE (1998) J Chem Phys 109(2):400
266. Kanai Y, Wang X, Selloni A, Car R (2006) J Chem Phys 125:234104
267. Perdew JP, Ruzsinszky A, Constantin LA, Csonka GI, Sun J (2009) Phys Rev Lett 103:026403
268. Zhao Y, Truhlar DG (2006) J Chem Phys 125:194101
269. Zhao Y, Truhlar DG (2008) Theor Chem Acc 120:215
270. Madsen GKH, Ferrighi L, Hammer B (2010) J Phys Chem Lett 1:515
271. Sun J, Xiao B, Ruzsinszky A (2012) J Chem Phys 137:051110
272. Sun J, Haunschild R, Xiao B, Bulik I, Scuseria GE, Perdew JP (2013) J Chem Phys 138:044113
273. Sun J, Xiao B, Fang Y, Haunschild R, Hao P, Ruzsinszky A, Csonka GI, Scuseria GE, Perdew JP (2013) Phys Rev Lett 111:106401
274. Peverati R, Truhlar DG (2012) J Phys Chem Lett 3:117
275. Wheeler SE, Houk KN (2010) J Chem Theory Comput 6:395

276. Ferrighi L, Madsen GKH, Hammer B (2011) J Chem Phys 135:084704
277. Andersen M, Hornekær L, Hammer B (2012) Phys Rev B 86:085405
278. Marom N, Tkatchenko A, Rossi M, Gobre VV, Hod O, Scheffler M, Kronik L (2011) J Chem Theory Comput 7(12):3944
279. Balog R, Andersen M, Jrgensen B, Sljivancanin Z, Hammer B, Baraldi A, Larciprete R, Hofmann P, Hornekr L, Lizzit S (2013) ACS Nano 7:3823
280. Grns E, Andersen M, Arman MA, Gerber T, Hammer B, Schnadt J, Andersen JN, Michely T, Knudsen J (2013) J Phys Chem C 117(32):16438
281. Zhu M, Aikens CM, Hollander FJ, Schatz GC, Jin R (2008) J Am Chem Soc 130(18):5883
282. Ferrighi L, Pan YX, Grönbek H, Hammer B (2012) J Phys Chem C 116:7374
283. Luo S, Zhao Y, Truhlar DG (2012) J Phys Chem Lett 3:2975
284. Sun J, Marsman M, Ruzsinszky A, Kresse G, Perdew JP (2011) Phys Rev B 83:121410
285. Batista ER, Heyd J, Hennig RG, Uberuaga BP, Martin RL, Scuseria GE, Umrigar CJ, Wilkins JW (2006) Phys Rev B 74:121102(R)
286. El-Mellouhi F, Brothers EN, Lucero MJ, Scuseria GE (2013) J Phys Condens Matter 25:135501
287. Paier J, Penschke C, Sauer J (2013) Chem Rev 113:3949
288. Penschke C, Paier J, Sauer J (2013) J Phys Chem C 117:5274
289. Papageorgiou AC, Beglitis NS, Pang CL, Teobaldi G, Cabailh G, Chen Q, Fisher AJ, Hofer WA, Thornton G (2010) Proc Natl Acad Sci 107(6):2391
290. Teobaldi G, Tanimura K, Shluger AL (2010) Phys Rev B 82:174104
291. Pacchioni G (2008) J Chem Phys 128:182505
292. Vilhelmsen LB, Walton KS, Sholl DS (2012) J Am Chem Soc 134:12807
293. Yadnum S, Choomwattana S, Khongpracha P, Sirijaraensre J, Limtrakul J (2013) ChemPhysChem 14:923
294. Valero R, Gomes JRB, Truhlar DG, Illas F (2008) J Chem Phys 129:124710
295. Valero R, Gomes JRB, Truhlar DG, Illas F (2010) J Chem Phys 132:104701
296. Paier J, Marsman M, Kresse G (2007) J Chem Phys 127:024103
297. Lynch BJ, Truhlar DG (2003) J Phys Chem A 107:8996, 108:1460(E) (2004)
298. Bealing CR, Ranprasad R (2013) J Chem Phys 139:174904
299. Fu Q, Saltzburg H, Flytzani-Stephanopoulos M (2003) Science 301:935
300. Lu W, Filimonov SN, Carrasco J, Tkatchenko A (2013) Nat Commun 4:2569
301. Civarelli B, Zicovich-Wilson CM, Valenzaon L, Ugliengo P (2008) Cryst Eng Comm 10:405
302. Zicovich-Wilson CM, Kirtman B, Civalleri B, Ramírez-Solís A (2010) Phys Chem Chem Phys 12:3289
303. Civarelli B, Maschio L, Ugliengo P, Zicovich-Wilson CM (2010) Phys Chem Chem Phys 12:6382
304. Leverentz HR, Qi HW, Truhlar DG (2013) J Chem Theory Comput 9(2):995
305. Aguero A, Janesko BG (2012) J Chem Phys 136:024111
306. Janesko BG (2013) In J Quant Chem 113:83